

Zero-Forcing Beamforming Energy Efficiency Optimization for the Security Control of Wireless Power Transfer System

Zhimeng Xu*, Jinyu Chen, Fenli Qiu, and Yisheng Zhao

Abstract—This paper proposes a zero-forcing beamforming design for the energy efficiency optimization of the magnetic resonance based wireless power transfer system with multiple transmitter coils, which aims to secure energy transfer control. A scheme based on beamforming technology is proposed to prevent unauthorized users from accessing the system, which builds a beamforming model consisting of multiple transmitter coils, a target receiver, and a non-target receiver to simulate the actual system. Then to optimize the proposed system's energy efficiency while constraining the target receiver's energy, spectral efficiency, and transmitter's power, the proposed beamforming model is constructed as an optimization problem. To solve this non-convex nonlinear fractional programming problem, the Dinkelbach algorithm is used for fractional conversion, and then the zero-forcing constraints are equivalently replaced. Finally, two solutions of the nonlinear solution and closed-form solution are derived. The simulation results show that the energy efficiency optimization strategies of zero-forcing beamforming with the two derived solutions can satisfy the design requirements.

1. INTRODUCTION

Magnetic Resonance Coupling (MRC) is widely used in Wireless Power Transfer (WPT) systems for its high energy transfer efficiency and low radiation [1]. In the current WPT system, the transmitter and receiver coils must be aligned and fit together to ensure that the system achieves efficient energy transfer. To solve this problem, the application of multiple transmitter coils and beamforming technology has attracted great attention from worldwide scholars.

To prevent unauthorized users from accessing the system, in [2] the expected receiver power was maximized by optimizing the current of transmitters to meet the power constraint of the transmitter's transfer power and unexpected receivers' power, which realized the security power transfer. On this basis, to increase the expected received power, in [3] the system design was converted into an optimization problem, which maximized the expected receiver power by optimizing the turns of the coil in the magnetic resonance circuit, and used semi-definite relaxation to optimize the solution. Consider that the recent wireless charging devices need wireless charging protocol to guarantee the security power transfer, which means that the transmitter needs to communicate with the receiver before energy transfer. In general, most of the wireless charging systems use the same coil of energy transmission for information transmission to simplify the system design. Therefore, in this kind of wireless charging system that needs authorization, information transmission should also be considered. Accordingly, the previous methods mentioned above only consider the optimization of energy transfer, which cannot be applied and needs further research.

This paper proposes an energy efficiency optimization method based on zero-forcing beamforming technology for the WPT system requiring authorization. Referring to the simultaneous wireless information and power (SWIPT) technology, the mentioned WPT system in this paper transmits energy

Received 8 May 2021, Accepted 20 July 2021, Scheduled 22 July 2021

* Corresponding author: Zhimeng Xu (zhmxu@fzu.edu.cn).

The authors are with the College of Physics and Information Engineering, Fuzhou University, Fuzhou 350108, China.

and information to the receiver under power splitting, and it is built as a beamforming model containing multiple transmitters, a target receiver, and a non-target receiver. A transmission controller is designed to communicate with the transmitters and receivers and to adjust the voltage of the transmitter in real-time. In this system model, the zero-forcing beamforming design is converted to an optimization problem, to maximize energy efficiency, while constraining the transmitter power, target receiver energy, and spectral efficiency. By solving the optimization problem, a zero-forcing beamforming energy efficiency optimization design strategy is obtained.

2. MODELS AND ANALYSIS

2.1. System Model

The system model is shown in Fig. 1(a), which contains a target receiver (RX_1), a non-target receiver (RX_2), and multiple transmitters (TX_i , $n = 1, 2 \dots N$) powered by sinusoidal voltage source with amplitude v_p and phase φ_p [4]. A transmission controller is used to not only communicate with the transmitter and receiver but also adjust the voltage in the transmitter and the resonance capacitance of the transceiver in real-time [5]. Assume that the capacitance, resistance, and self-inductance of transmitter are C_n, r_n, L_n ($n = 1, 2 \dots N$), respectively, and the resistance of the q -th receiver $r_{r,q} = r_{p,q} + r_{l,q}$, $q = 1, 2$, where $r_{p,q}, r_{l,q}$ are the parasitic resistance and load resistance of the q -th receiver respectively, and $r_{l,q} \gg r_{p,q}$. When the circuit works in resonance, the system can achieve efficient transfer, and the system resonance frequency can be expressed [4] as:

$$\omega = 2\pi f = \frac{1}{\sqrt{L_n C_n}} = \frac{1}{\sqrt{L_{r,q} C_{r,q}}} \quad (1)$$

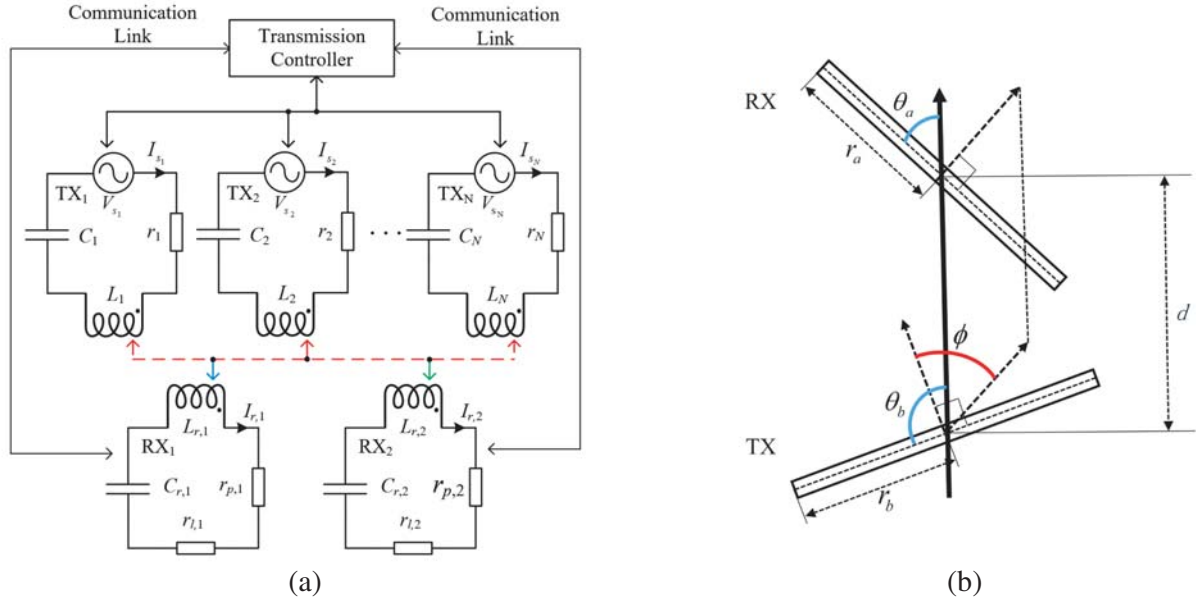


Figure 1. (a) System Model. (b) Angle and position between coils.

The coupling effect between the transceiver coils, which can be denoted by mutual inductance, is directly related to the shape and size of the coil, the number of turns, and the placement position. Therefore, the mutual inductance can be expressed [6, 7] as:

$$M = \mu\pi N_a N_b \frac{r_a^2 r_b^2}{4d^3} (2 \sin \theta_a \sin \theta_b + \cos \theta_a \cos \theta_b \cos \phi) \quad (2)$$

where $\mu = 4\pi \times 10^{-7} N/A^2$, and it is the vacuum permeability. N_a and N_b are the turns of coil a and coil b , respectively, which generate mutual inductance. r_a and r_b are the radii of coil a and coil b ,

respectively. d is the distance between two coils. θ_a and θ_b are the angles down from the line connecting the TX and RX coil centers to the radial directions of TX and RX coils, respectively, and ϕ is the angle between the radial directions of TX and RX coils, as shown in Fig. 1(b). For the multi-transceiver system, $M_{n,q}$ is defined as the mutual inductance between the n -th transmitter and the q -th receiver, and M_{nm} is defined as the mutual inductance between the n -th transmitter and the m -th transmitter, and $n \neq k$.

In addition, the receiver adopts the power distribution method [8], and its working method is to divide the received signal into two parts through the energy distributor. The power of part ρ is used for energy harvesting, and the power of part $(1 - \rho)$ is used for information decoding, where ρ is the power allocation factor, and $0 \leq \rho \leq 1$.

2.2. Circuit Analysis

When the system is in the magnetic resonance coupling state, the impedance of the transmitter is resistive, that is, the impedance of the transmitter $Z_n = r_n$ ($n = 1, 2, \dots, N$), and the impedance of receiver $Z_{r,q} = r_{r,q}$ ($q = 1, 2$). Ignoring the mutual inductance between the receivers, according to Kirchhoff's voltage law [8], the current of the q -th receiver and the voltage of the n -th transmitter can be simplified to:

$$I_{r,q} = \frac{j\omega}{r_{r,q}} (M_{1,q}I_{s_1} + M_{2,q}I_{s_2} + \dots + M_{n,q}I_{s_N}) \quad (3)$$

$$V_{s_n} = r_n I_{s_n} + j\omega \sum_{m=1, \neq n}^N M_{nm} I_{s_m} - j\omega \sum_{q=1}^2 M_{n,q} I_{r,q} \quad (4)$$

Combining Eq. (3) and Eq. (4), the voltage of the n -th transmitter can be further obtained as:

$$V_{s_n} = \left(r_n + \sum_{q=1}^2 \frac{\omega^2 M_{n,q}^2}{r_{r,q}} \right) I_{s_n} + \sum_{m \neq n}^N \left(j\omega M_{nm} + \sum_{q=1}^2 \frac{\omega^2 M_{n,q} M_{q,m}}{r_{r,q}} \right) I_{s_m} = v_p e^{j\varphi_p} \quad (5)$$

From Eq. (5), the voltage of the n -th transmitter can be derived from the transmitter currents. To simplify the analysis, the transfer currents will be first derived in the following beamforming analysis, and then it will be converted into the specific requirements of the voltage source.

2.3. Beamforming Analysis

The beamforming signal comes from the current signal of the transmitter, and the transfer signal can be expressed [9] as:

$$\mathbf{I}_S = \mathbf{i} * s \quad (6)$$

where the beamforming vector, also the transmitter current, is defined as $\mathbf{i} = [I_{s_1}, I_{s_2}, \dots, I_{s_N}]^T$, and the transfer symbol is defined as $s \sim \mathcal{CN}(0, 1)$.

From Eq. (3), the beamforming signal received by the receiver can be reexpressed as:

$$I_{r,q} = \mathbf{m}_q^H \mathbf{I}_S + n_q \quad (7)$$

where $n_q \sim \mathcal{CN}(0, \sigma_q^2)$, and it is the complex additive white Gaussian noise of the q -th receiver. $\mathbf{m}_q = \frac{j\omega}{r_{r,q}} [M_{1,q}, M_{2,q} \dots M_{N,q}]^T$, and it is the mutual inductance coefficient vector between the q -th receiver and all transmitters.

After power splitting, the current expressions for information decoding and energy harvesting of the target receiver RX_1 can be expressed [10] as:

$$I_{r,I_1} = \sqrt{1 - \rho_1} (\mathbf{m}_1^T \mathbf{I}_S + n_1) + n_{a_1} \quad (8)$$

$$I_{r,E_1} = \sqrt{\rho_1} (\mathbf{m}_1^T \mathbf{I}_S + n_1) \quad (9)$$

where $na_1 \sim \mathcal{CN}(0, \delta_1^2)$, and it is the additive white Gaussian noise caused by the information decoding side of the target receiver. Then the power obtained by information decoding and energy harvesting of the target receiver RX_1 can be obtained as:

$$\begin{aligned} P_{I,1} &= \frac{1}{2}|I_{r,I_1}|^2 r_{l,1} \\ &= \frac{1}{2} \left| \sqrt{(1-\rho_1)} (\mathbf{m}_1^T \mathbf{i} s + n_1) + z_1 \right|^2 r_{l,1} \\ &= \frac{1}{2} r_{l,1} [(1-\rho_1) (\mathbf{i}^H \mathbf{m}_1 \mathbf{m}_1^T \mathbf{i} + \sigma_1^2) + \delta_1^2] \end{aligned} \quad (10)$$

$$\begin{aligned} P_{E,1} &= \frac{1}{2}|I_{r,E_1}|^2 r_{l,1} \\ &= \frac{1}{2} \left| \sqrt{\rho_1} (\mathbf{m}_1^T \mathbf{i} s + n_1) \right|^2 r_{l,1} \\ &= \frac{1}{2} r_{l,1} \rho_1 (\mathbf{i}^H \mathbf{m}_1 \mathbf{m}_1^T \mathbf{i} + \sigma_1^2) \end{aligned} \quad (11)$$

According to Eq. (10), it is easy to obtain the signal-to-noise ratio of the target receiver (RX_1) as:

$$SNR_1 = \frac{(1-\rho_1) \left(\frac{r_{l,1}}{2} \mathbf{i}^H \mathbf{m}_1 \mathbf{m}_1^T \mathbf{i} \right)}{(1-\rho_1) \sigma_1^2 + \delta_1^2} \quad (12)$$

From Shannon's formula, the spectral efficiency of the target receiver RX_1 is obtained as:

$$\beta_1 = \log_2(1 + SNR_1) \quad (13)$$

Then the power of the n -th transmitter and the total power provided by n transmitters can be reexpressed as:

$$P_n = \frac{1}{2} \mathbf{i}^H \mathbf{D}_n \mathbf{i}, \quad n = 1, 2, \dots, N \quad (14)$$

$$P_S = \frac{1}{2} \mathbf{i}^H \left(\mathbf{R} + \sum_{q=1}^2 r_{r,q} \mathbf{m}_q \mathbf{m}_q^T \right) \mathbf{i} = \frac{1}{2} \mathbf{i}^H \mathbf{B}_1 \mathbf{i} \quad (15)$$

where

$$\begin{aligned} \mathbf{R} &= \text{diag} \{r_1, r_2, \dots, r_N\}, \\ \mathbf{D}_n(i, j) &= \begin{cases} r_n, & \text{if } i = j = n \\ 0, & \text{else} \end{cases}, \\ \mathbf{B}_1 &= \mathbf{R} + \sum_{q=1}^2 r_{r,q} \mathbf{m}_q \mathbf{m}_q^T. \end{aligned}$$

From Eq. (11) and Eq. (15), the total power consumption of the system can be further obtained as:

$$P_{total} = P_S + P_C - P_{E,1} \quad (16)$$

where P_C is the constant power consumption of the circuit caused by signal processing. Unlike common wireless communication systems, the power consumption of the WPT system based on magnetic resonance can be compensated by the transmitted energy [11].

3. MODELING AND SOLVING PROBLEMS

3.1. Modeling of Zero-Forcing Beamforming Problem

The system energy efficiency [10] is introduced to balance the relationship between spectral efficiency and total system power consumption, which is expressed as $\eta = \frac{\beta_1}{P_{total}}$. To guarantee the receiver's service

quality and high-efficiency energy transfer, the situation is described as an optimization problem with the goal of maximizing the energy efficiency of the target receiver (RX_1), which satisfies the two constraints that the acquired energy is greater than the value of energy threshold, and the spectral efficiency is greater than the preset value of the spectral efficiency of the information decoding part; and that the total power of the transmitter is less than the maximum of total transfer power and the power of each transmitter is less than the transfer power threshold. Besides, the zero-forcing constraint is added, considering the two possible situations that the non-target receiver (RX_2) steals the energy and private information of the target receiver (RX_1) without paying, and there is no need to transmit power and information to RX_2 . Assume that the magnetic resonance zero-forcing beamforming scheme is adopted by the transmission controller. After abstracting the actual problem, the optimization problem $P0$ can be expressed as:

$$P0 : \max_{\mathbf{i}} \frac{\log_2 \left(1 + \frac{\frac{1}{2}(1-\rho_1)r_{l,1}\mathbf{i}^H\mathbf{m}_1\mathbf{m}_1^T\mathbf{i}}{(1-\rho_1)\sigma_1^2 + \delta_1^2} \right)}{\frac{1}{2}\mathbf{i}^H\mathbf{B}_1\mathbf{i} + P_C - P_{E,1}} \quad (17)$$

$$s.t. \quad \rho_1 \left(\frac{1}{2}r_{l,1}\mathbf{i}^H\mathbf{m}_1\mathbf{m}_1^T\mathbf{i} + \sigma_1^2 \right) \geq e_1 \quad (18)$$

$$\log_2 \left(1 + \frac{\frac{1}{2}(1-\rho_1)r_{l,1}\mathbf{i}^H\mathbf{m}_1\mathbf{m}_1^T\mathbf{i}}{(1-\rho_1)\sigma_1^2 + \delta_1^2} \right) \geq v_1 \quad (19)$$

$$\frac{1}{2}\mathbf{i}^H\mathbf{B}_1\mathbf{i} \leq P_m \quad (20)$$

$$\frac{1}{2}\mathbf{i}^H\mathbf{D}_n\mathbf{i} \leq P_{t,n}, \quad n = 1, 2, \dots, N \quad (21)$$

$$\mathbf{m}_2^T\mathbf{i} = 0 \quad (22)$$

where e_1 , v_1 , P_m , $P_{t,n}$ are the energy threshold of energy receiving part of the target receiver, the minimum spectral efficiency of the information decoding part of the target receiver, the total transfer power threshold, and the minimum transfer power of the n -th transmitter respectively, and Eq. (22) is the constraint condition of magnetic resonance zero-forcing beamforming which means that the mutual inductance vector of the non-target receiver and the current vector of the transmitter are orthogonal to each other, and ensures that the non-target receiver will not cause any interference to the target receiver. Since Eq. (19) is a log function, it can be converted as:

$$\frac{\frac{1}{2}(1-\rho_1)r_{l,1}\mathbf{i}^H\mathbf{m}_1\mathbf{m}_1^T\mathbf{i}}{(1-\rho_1)\sigma_1^2 + \delta_1^2} \geq 2^{v_1} - 1 \quad (23)$$

Obviously, the objective function of problem $P0$ is a complex fractional programming problem, and it is difficult to judge its unevenness. Thus, we will focus on how to solve this problem in the next section.

3.2. Optimization Problem Solving

3.2.1. Dinkelbach Algorithm

The objective function of problem $P0$ can be converted into an integral programming problem which is easy to measure its concavity and convexity by the Dinkelbach algorithm. The Dinkelbach algorithm [13] is similar to Newton's iteration method in theory but is different from the dichotomy method. The idea is to first set an initial value, and then continuously move the value according to a better solution, and finally approach the optimal solution step by step. Therefore, through the Dinkelbach algorithm, the

objective function can be equivalent to:

$$\max_{\mathbf{i}} \log_2 \left(1 + \frac{\frac{1}{2}(1-\rho_1)r_{l,1}\mathbf{i}^H\mathbf{m}_1\mathbf{m}_1^T\mathbf{i}}{(1-\rho_1)\sigma_1^2 + \delta_1^2} \right) - \eta \left(\frac{1}{2}\mathbf{i}^H\mathbf{B}_1\mathbf{i} + P_C - P_{E,1} \right) \quad (24)$$

Note that the problem after conversion is still a non-convex quadratic constrained quadratic programming optimization problem. Although the optimal solution can be obtained by combining semi-definite relaxation and Dinkelbach's algorithm, its computational complexity is high, and it is not suitable for providing real-time solutions. Thus, the problem will be further converted.

3.2.2. Conversion of Zero-Forcing Constraints

The constraint condition Eq. (22) is converted by expressions $\mathbf{i}_0 = \frac{\mathbf{v}_2\mathbf{v}_2^H\mathbf{m}_1}{\|\mathbf{v}_2\mathbf{v}_2^H\mathbf{m}_1\|}$ and $h_1 = |\mathbf{m}_1^T\mathbf{i}_0|^2$, where \mathbf{v}_2 is the orthogonal basis of the mutual inductance vector \mathbf{m}_2 in the null space [12]. Assuming that $\mathbf{i} = \sqrt{k_1}\mathbf{i}_0$, $b_1 = \mathbf{i}_0^H(\mathbf{R} + \sum_{q=1}^2 r_{r,q}\mathbf{m}_q\mathbf{m}_q^T)\mathbf{i}_0$, and $d_n = \mathbf{i}_0^H\mathbf{D}_n\mathbf{i}_0$ ($n = 1, 2, \dots, N$), the converted problem $P1$ can be written as:

$$P1: \quad \max_{\mathbf{i}} \log_2 \left(1 + \frac{\frac{1}{2}(1-\rho_1)r_{l,1}\mathbf{i}^H\mathbf{m}_1\mathbf{m}_1^T\mathbf{i}}{(1-\rho_1)\sigma_1^2 + \delta_1^2} \right) - \eta \left(\frac{1}{2}\mathbf{i}^H\mathbf{B}_1\mathbf{i} + P_C - P_{E,1} \right) \quad (25)$$

$$s.t. \quad \rho_1 \left(\frac{1}{2}r_{l,1}k_1h_1 + \sigma_1^2 \right) \geq e_1 \quad (26)$$

$$\frac{\frac{1}{2}r_{l,1}(1-\rho_1)k_1h_1}{(1-\rho_1)\sigma_1^2 + \delta_1^2} \geq 2^{v_1} - 1 \quad (27)$$

$$\frac{1}{2}b_1k_1 \leq P_m \quad (28)$$

$$\frac{1}{2}d_nk_1 \leq P_{t,n}, \quad n = 1, 2, \dots, N \quad (29)$$

Note that, by observing the structure of problem $P1$, all the constraints of the problem are convex sets, and closed space is formed, while the objective function is a concave function. Based on the analysis above, the following two solutions can be proposed.

3.2.3. Nonlinear Solution (NLS)

The problem $P1$ is a convex optimization problem constrained to be a convex set. To further simplify the notation, assume that $g_1 = \frac{2(\frac{e_1}{\rho_1} - \sigma_1^2)}{r_{l,1}h_1}$, $l_n = \frac{2P_{t,n}}{d_n}$ ($n = 1, 2, \dots, N$), $g_2 = \frac{2(2^{v_1} - 1)((1-\rho_1)\sigma_1^2 + \delta_1^2)}{r_{l,1}(1-\rho_1)h_1}$, and $P_{\max} = \frac{2P_m}{b_1}$ respectively. Then the converted problem $P2$ can be expressed as:

$$P2: \quad \max_{k_1} \log_2 \left(1 + \frac{\frac{1}{2}r_{l,1}(1-\rho_1)k_1h_1}{(1-\rho_1)\sigma_1^2 + \delta_1^2} \right) - \eta \left(\frac{1}{2}b_1k_1 + P_C - P_{E,1} \right) \quad (30)$$

$$s.t. \quad k_1 \geq g_1 \quad (31)$$

$$k_1 \geq g_2 \quad (32)$$

$$k_1 \leq P_{\max} \quad (33)$$

$$k_1 \leq l_n, \quad n = 1, 2, \dots, N \quad (34)$$

Undoubtedly, $P2$ is a nonlinear convex programming problem with linear constraints, so it can be solved directly by the CVX toolkit [14] in convex optimization.

3.2.4. Closed-Form Solution (CFS)

Observing the structure of problem $P1$, we note that the constraints Eq. (26), Eq. (27), Eq. (28), and Eq. (29) form a closed space. According to this, problem $P1$ can be solved by considering all possible situations. After first-order derivation of the objective function, the Stationary Point (SP) of the objective function is obtained as:

$$k_1^{SP} = \frac{1}{\frac{1}{2}b_1\eta - \frac{1}{2}\eta\rho l_{l,1}h_1} - \frac{(1 - \rho_1)\sigma_1^2 + \delta_1^2}{\frac{1}{2}(1 - \rho_1)h_1r_{l,1}} \quad (35)$$

$P2$ is a univariate convex problem with bounded constraints, and the optimal value must be on the constraint boundary or at the SP. Then by comparing the five values of P_{\max} , k_1^{SP} , g_1 , g_2 , and $\min(l_n, n = 1, 2 \dots N)$, the optimal solution of the problem is obtained. P_{\max} is the optimal solution to the problem when P_{\max} is less than the SP k_1^{SP} and $\min(l_n, n = 1, 2 \dots N)$, and the SP k_1^{SP} is the optimal solution to the problem when P_{\max} grows to be greater than or equal to the SP k_1^{SP} , and the SP k_1^{SP} is less than or equal to $\min(l_n, n = 1, 2 \dots N)$ and $\max(g_1, g_2)$. The conversion problem $P3$ is shown below:

$$P3: \quad k_1 = \begin{cases} k_1^{SP}, & \text{if } P_{\max} \geq k_1^{SP} \geq \max(g_1, g_2) \text{ and } k_1^{SP} \leq \min(l_n, n = 1, 2, \dots, N); \\ P_{\max}, & \text{if } k_1^{SP} \geq P_{\max} \geq \max(g_1, g_2) \text{ and } k_{\max} \leq \min(l_n, n = 1, 2, \dots, N); \\ g_1, & \text{if } P_{\max} \geq g_1 \geq \max(k_1^{SP}, g_2) \text{ and } g_1 \leq \min(l_n, n = 1, 2, \dots, N); \\ g_2, & \text{if } P_{\max} \geq g_2 \geq \max(g_1, k_1^{SP}) \text{ and } g_2 \leq \min(l_n, n = 1, 2, \dots, N); \\ \min(l_n, n = 1, 2, \dots, N), & \text{else.} \end{cases} \quad (36)$$

4. SIMULATION RESULTS AND DISCUSSION

4.1. Parameter Setting

The simulation in this section will evaluate the performance of the proposed magnetic resonance beamforming strategy of the WPT system. In the simulation, the resonance frequency of the system is selected as $\omega = 6.78 \times 10^6$ rad/s; the $N = 5$ transmitters are placed in $(0, 0, 0)$ m, $(0.6, 0.6, 0)$ m, $(-0.6, 0.6, 0)$ m, $(-0.6, -0.6, 0)$ m, $(0.6, -0.6, 0)$ m; the target receiver RX_1 is placed at $(0.3, 0.3, 0.1)$ m; and the other non-target receiver RX_2 is placed at $(-0.3, 0.3, 0.1)$ m. The coils are all made of copper wire with a cross-sectional radius of 0.8 mm. Each transmitter is 200 turns, and the diameter of the coil is 0.2 m. Each receiver is 100 turns, and the diameter of the coil is 0.04 m. After setting the above parameters, the mutual inductance between the coils can be calculated separately. The transmitter resistance and receiver parasitic resistance can be calculated by [5] to be 1.05Ω and 0.105Ω , respectively. Assuming that the constant power consumption of the circuit is $P_C = 300$ mW, the noise power is $\sigma_1^2 = \delta_1^2 = -10$ dBm; the transfer power threshold is $P_n = 22$ dBm, $n = 1, 2 \dots N$; and the load resistance is 50Ω . The Spectral Efficiency Maximization (SEM) [15] scheme, the beam-domain SWIPT protocol for mMIMO system with non-linear Energy Harvesting (NL-EH) [16], and the secure energy-efficiency resource allocation (SERA) [17] algorithm are taken as the benchmarks.

4.2. Simulation Analysis

First, the impact of the power splitting factor ρ on the energy efficiency of the system is analyzed. Assuming that the energy threshold $e_1 = 10$ dBm, the spectral efficiency constraint $v_1 = 1$ bps/Hz, and the total transfer power threshold $P_S = 30$ dBm. Observing Fig. 2(a), with the increase of ρ , the proposed optimization scheme is always better than the SEM. The value of system energy efficiency is related to the value of ρ , because the change of ρ directly affects the ratio of energy harvesting and information decoding of the target receiver. When ρ increases to 0.3, the energy efficiency of the proposed optimization scheme reaches the highest value, and the energy efficiencies of the NLS scheme and CFS scheme are the same, while the SEM begins to gradually decrease as ρ increases to 0.6. Therefore, in the subsequent simulation, the power splitting factor ρ is set to 0.3.

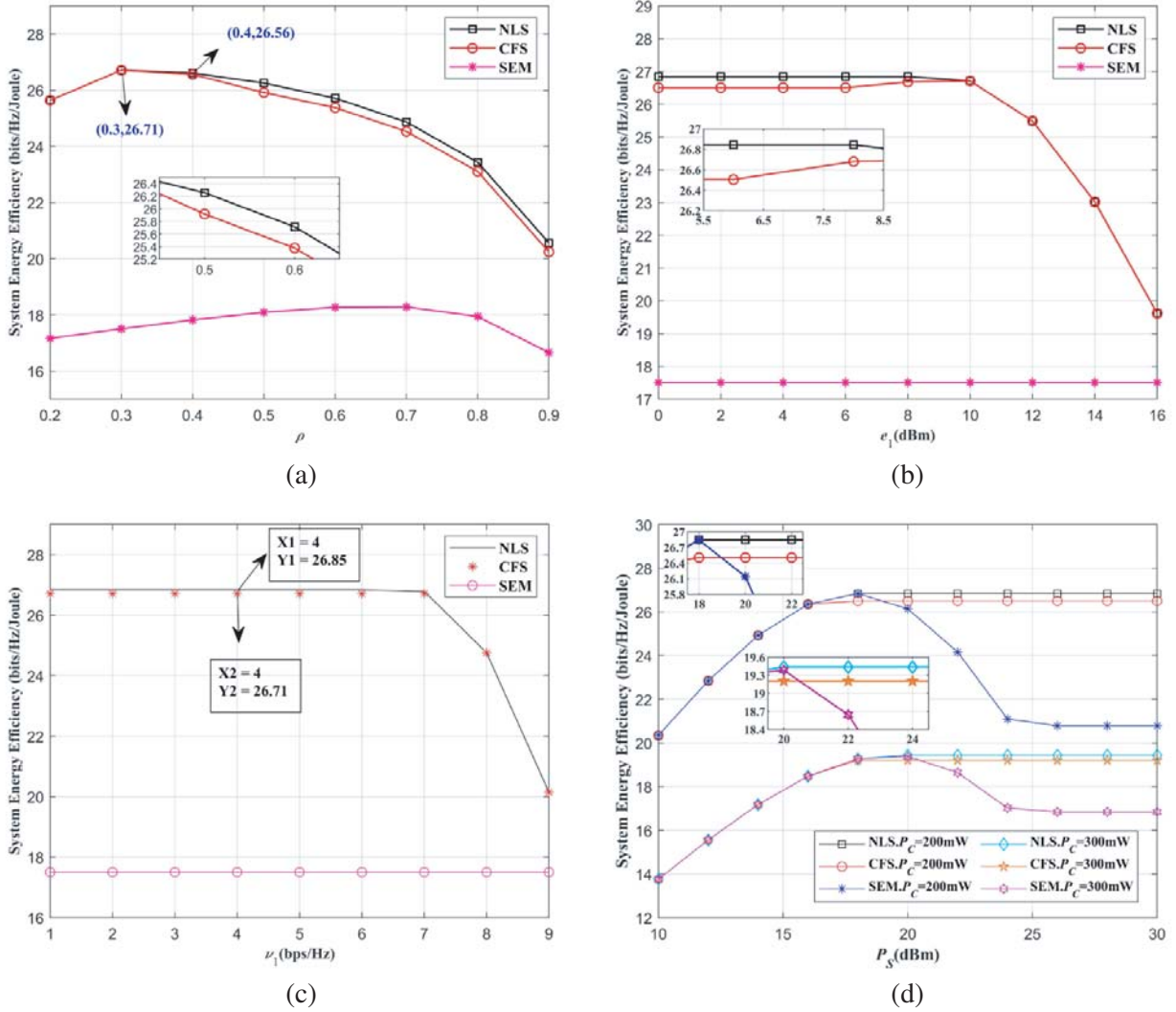


Figure 2. (a) System energy efficiency versus power splitter ratio ρ . (b) System energy efficiency versus energy threshold. (c) System energy efficiency versus minimum spectral efficiency threshold. (d) System energy efficiency versus total transfer power threshold.

To explain how the proposed strategy works in practice, two scenarios when $\rho = 0.3$ and $\rho = 0.9$ are investigated. The optimal solution k_1^* of NLS and the corresponding voltage of all TXs are given in Table 1. The position information of each coil is obtained by wireless link connected to the transmission controller. It can be calculated by Eq. (2) to obtain M , and then the optimal solution can be obtained by the built-in convex optimization program and converted into \mathbf{i} , and further converted into corresponding physical parameters by Eq. (5). The power obtained by the energy harvesting of the receiver is shown in Table 1. The numerical results show that $P_{E,2}^*$ of the non-target receiver is close to zero due to the zero-forcing beamforming.

Then, the energy thresholds e_1 and system energy efficiencies under different schemes are compared, as shown in Fig. 2(b). Let the spectral efficiency constraint $\nu_1 = 1$ bps/Hz and the total transfer power threshold $P_S = 30$ dBm. It can be seen that the energy efficiency of the NLS scheme is slightly higher than that of the CFS scheme when $e_1 \leq 8$ dBm, and the energy efficiencies of the two schemes are always better than the SEM. When the energy threshold is $e_1 > 8$ dBm, the values of energy efficiency obtained by the NLS scheme and CFS scheme begin to decline, and the benchmark never changes with the increase of e_1 . The reason is that e_1 exceeds the energy corresponding to the best energy efficiency

Table 1. Optimal solutions of NLS under different power splitting factor (V, rad, dBm).

	$\rho = 0.3$	$\rho = 0.9$
k_1^*	0.0814	0.1211
$(V_{s_1}^*, v_{p_1}^*, \varphi_{p_1}^*)$	(0.3104 + 5.4938i, 5.5026, 1.5143)	(0.3786 + 6.7002i, 6.7109, 1.5143)
$(V_{s_2}^*, v_{p_2}^*, \varphi_{p_2}^*)$	(0.4530 + 2.7094i, 2.7470, 1.4051)	(0.5525 + 3.3044i, 3.3502, 1.4051)
$(V_{s_3}^*, v_{p_3}^*, \varphi_{p_3}^*)$	(-0.1094 + 8.0445i, 8.0452, 1.5844)	(-0.1334 + 9.8110i, 9.8119, 1.5844)
$(V_{s_4}^*, v_{p_4}^*, \varphi_{p_4}^*)$	(0.0041 + 4.0255i, 4.0255, 1.5698)	(0.0050 + 4.9095i, 4.9095, 1.5698)
$(V_{s_5}^*, v_{p_5}^*, \varphi_{p_5}^*)$	(0.0431 + 7.2493i, 7.2494, 1.5649)	(0.0525 + 8.8412i, 8.8414, 1.5649)
$(P_{E,1}^*, P_{E,2}^*)$	(10.000, -15.228)	(16.493, -10.457)

value obtained by the proposed scheme. The total transfer power will be increased to satisfy the energy constraint, which leads to a sudden decrease in energy efficiency. The SEM takes spectral efficiency as the objective function, and the optimal energy obtained by using the optimal spectral efficiency obtained by the solution is always above the minimum energy threshold.

Figure 2(c) shows the relationship between the spectral efficiency threshold v_1 and the system energy efficiency under different schemes. Assume that the power splitting factor $\rho = 0.3$, the energy constraint $e_1 = 10$ dBm, and the total transfer power threshold $P_S = 30$ dBm. It can be found that, with the increase of the spectral efficiency threshold v_1 , the energy efficiencies of the two proposed schemes are similar, while the performance of the SEM remains unchanged and is always lower than the proposed optimization scheme. The energy efficiencies of the two proposed optimization schemes begin to decline when v_1 increases to 7 bps/Hz, because v_1 exceeds the spectral efficiency corresponding to the optimal energy efficiency value. In this case, in order to satisfy the spectral efficiency constraint, it is necessary to increase the total transfer power which leads to a sharp drop in energy efficiency.

Last, the relationship between the total transfer power threshold P_S and the system energy efficiency is analyzed. Assume that the power splitting factor $\rho = 0.3$, the minimum spectral efficiency $v_1 = 1$ bps/Hz, and the energy threshold $e_1 = 10$ dBm. From Fig. 2(d), it can be known that the larger the P_C is, the worse the performance of the system's energy efficiency is. The energy efficiencies of the two proposed schemes are consistent with that of the SEM when $P_C = 200$ mW and $P_S \leq 18$ dBm. At the critical point $P_S = 18$ dBm, the energy efficiency of the CFS scheme is slightly lower than that of the SEM and NLS schemes, because the SEM scheme is implemented on the basis of the NLS scheme. Then, as P_S continues to increase, the energy efficiency of the NLS solution remains unchanged, because the transfer power does not change. The performance of the CFS solution remains unchanged after a slight decline, while the benchmark solution remains stable after a gradual decline. The reason is that the scheme always uses full power for transfer at the beginning, and the performance drops sharply as the P_S increases. Then, the transfer power threshold of the n -th transmitter $P_{t,n}$ limits the increase of the actual transfer power P_S .

To further indicate the superiority of the proposed strategy, four methods are investigated in the following. Assume that $\rho = 0.3$, $v_1 = 1$ bps/Hz, $P_C = 200$ mW and $e_1 = 10$ dBm. The system

Table 2. Comparison of system energy efficiency under different method (bits/Hz/Joule).

P_S	NLS	CFS	NL-EH	SERA
10 dBm	20.3	20.3	1.2	9.5
15 dBm	25.8	25.8	2.8	9.3
20 dBm	26.8	26.5	5.3	11.2
25 dBm	26.8	26.5	9.6	15.6
30 dBm	26.8	26.5	17.6	19.6
35 dBm	26.8	26.5	28.9	20.9

energy efficiencies of the four methods in different P_S are given in Table 2. When $P_S \leq 30$ dBm, the system energy efficiencies of NLS and CFS are both higher than NL-EH and SERA. This shows that the proposed strategy can work more effectively in some information-carrying WPT systems with low-power transmitters.

5. CONCLUSIONS

This paper designs a zero-forcing beamforming strategy that maximizes energy efficiency in the application of the WPT system to prevent unauthorized users accessing the system privately. Based on the application background and design goals, the system is built as a beamforming model consisting of multiple transmitters, a target receiver, and a non-target receiver, and thereby the above beamforming design is converted to an optimization problem. Then, two optimal solutions of nonlinear solution and closed-form solution are obtained by the Dinkelbach algorithm and zero-forcing constraints. Last, through simulation analysis, it is verified that the energy efficiencies of the two optimal solutions are similar, and the proposed beamforming strategy can make the system energy efficiency higher than that of the benchmark scheme. It can be concluded that the proposed strategy can meet the requirements of the WPT system for energy security transfer control.

ACKNOWLEDGMENT

National Natural Science Foundation of China (No. 62071125), Natural Science Foundation of Fujian Province (No. 2018J01805), Industry-University-Research Collaboration Project of Fujian Province under Grant (No. 2019H6007) and Talent Foundation of Fuzhou University (No. GXRC-18083).

REFERENCES

1. Zhang, Z., H. Pang, and A. Georgiadis, "Wireless power transfer: An overview," *IEEE Transactions on Industrial Electronics*, Vol. 66, No. 2, 1044–1058, Feb. 2019.
2. Sun, H., H. Lin, and F. Zhu, "Magnetic resonant beamforming for secured wireless power transfer," *IEEE Signal Processing Letters*, Vol. 24, No. 9, 1173–1177, Aug. 2017.
3. Sun, H., F. Gao, and F. Zhu, "Inductor design of magnetic resonance coupled circuits for secured wireless power transfer," *IEEE International Conference on Communications*, 1–6, 2017.
4. Campi, T., S. Cruciani, and F. Palandrani, "Wireless power transfer charging system for AIMDs and pacemakers," *IEEE Transactions on Microwave Theory and Techniques*, Vol. 64, No. 2, 633–642, Feb. 2016.
5. Moghadam, M. R. and R. Zhang, "Multiuser wireless power transfer via magnetic resonant coupling: Performance analysis, charging control, and power region characterization," *IEEE Transactions on Signal and Information Processing over Networks*, Vol. 2, No. 1, 72–83, Mar. 2016.
6. Kisseleff, S., W. Gerstacker, and R. Schober, "Channel capacity of magnetic induction based wireless underground sensor networks under practical constraints," *IEEE Wireless Communication and Networking Conference*, 2603–2608, 2013.
7. Kisseleff, S., I. F. Akyildiz, and W. H. Gerstacker, "Throughput of the magnetic induction based wireless underground sensor networks: Key optimization techniques," *IEEE Transactions on Communications*, Vol. 62, No. 12, 4426–4439, Dec. 2014.
8. Yang, G., M. R. Moghadam, and R. Zhang, "Magnetic MIMO signal processing and optimization for wireless power transfer," *IEEE Transactions on Signal Processing*, Vol. 65, No. 11, 2860–2874, Jun. 2017.
9. Jadidian, J. and D. Katabi, "Magnetic MIMO: How to charge your phone in your pocket," *20th ACM Annual International Conference on Mobile Computing and Networking*, 495–506, 2014.
10. Peng, C., Q. Shi, and W. Xu, "Energy efficiency optimization for multi-user MISO SWIPT systems," *IEEE China Summit and International Conference on Signal and Information Processing*, 772–776, 2015.

11. Ng, D. W., E. S. Lo, and R. Schober, "Wireless information and power transfer: Energy efficiency optimization in OFDMA systems," *IEEE Transactions on Wireless Communications*, Vol. 12, No. 12, 6352–6370, Dec. 2013.
12. Timotheou, S., I. Krikidis, and G. Zheng, "Beamforming for MISO interference channels with QoS and RF energy transfer," *IEEE Transactions on Wireless Communications*, Vol. 13, No. 5, 2646–2658, May 2014.
13. Tang, J., J. Luo, and M. Liu, "Energy efficiency optimization for NOMA with SWIPT," *IEEE Journal of Selected Topics in Signal Processing*, Vol. 13, No. 3, 452–466, Jun. 2019.
14. Guimaraes, D. A., G. H. Floriano, and L. S. Chaves, "A tutorial on the CVX system for modeling and solving convex optimization problems," *IEEE Latin America Transactions*, Vol. 13, No. 5, 1228–1257, May 2015.
15. Chu, Z., Z. Zhu, and M. Johnston, "Simultaneous wireless information power transfer for MISO secrecy channel," *IEEE Transactions on Vehicular Technology*, Vol. 65, No. 9, 6913–6925, Sept. 2016.
16. Xu, K., M. Zhang, J. Liu, et al., "SWIPT in mMIMO system with non-linear energy-harvesting terminals: Protocol design and performance optimization," *EURASIP Journal on Wireless Communications and Networking*, 72, 2019.
17. Yang, X, Z. Wang, X. Wan, and Z. Fan, "Secure energy-efficient resource allocation algorithm of massive MIMO system with SWIPT. Electronics," *Electronics*, Vol. 9, No. 1, 20, 2020.